CREST LINES AND CORRELATION FILTER BASED LOCATION OF THE MACULA IN DIGITAL RETINAL IMAGES

C. Mariño, M. G. Penedo, S. Pena
VARPA Group, Faculty of Informatics, University of A Coruña, A Coruña, Spain

F. González
School of Medicine and Complejo Hospitalario Universitario of Santiago, University of Santiago de Compostela, Santiago de Compostela, Spain

Keywords: Creases, correlation filter, macula, optic disk, deformable model.

Abstract: The fovea is a spot located in the center of the macula, and responsible for sharp central vision. In this paper a method to detect the macula location and size is presented, as a first step towards the fovea location.In the first stage of the process, the retinal vessel tree is extracted through a crest line detector. Then, the main vessel arc is fitted to a parabolic curve using a polynomial fitting process, which will allow for the computation of the area where the optic disc is located. The last stage consists in the segmentation of the optic disc, by means of the combination of morphological operations and a deformable model. Then, following the morphological properties of the eye, the macula location and size is determined by means of a new correlation filter. Search with this filter is performed in a reduced area of interest, whose size and position is determined by means, again, of the morphological properties of the eye. The algorithm has proven to be fast and accurate in the set of test images, composed of 135 digital retinal images.

1 INTRODUCTION

The retinal fundus photographs are widely used in the diagnosis of eye diseases. Processing automatically a large number of retinal images can help ophthalmologists to increase the efficiency in medical environments were big numbers of patients must be treated. The optic disk is the brightest area in images that do not have large areas of exudates and it is a slightly oval disk. It is the entrance region of vessels and its detection is very important since it works as a landmark for the other features in the retinal image. The macula is a commonly visible as a hazy dark area. This is the area with the highest number of cones and rods per unit area.

There are many previous works on optic disk localization. Goldbaum et al. (Goldbaum et al., 1996) extract the main features of the eye fundus (optic disk, vessels, blobs and fovea), through the combination of several templates, which work separately on the image color channels. Pinz et al. (Pinz et al., 1998) also obtain a map of the human retina using retinal angiographies, obtaining very good results. Lalonde et al. (Lalonde et al., 2001) extract the optic disk using Hausdorff based template matching and pyramidal decomposition. It is neither sufficiently sensitive nor specific enough for clinical application. On the other hand, strategies based on active contours (Mendels et al., 1999; Lowell et al., 2004; Chanwimluang and Fan, 2004) are used to detect the optic disk boundary in retinal images. These techniques are very robust against noise but their main disadvantage is their high computational cost.

A method for detecting the macular center was presented by Sinthanayothin (Sinthanayothin et al., 1999). In this approach a template based algorithm was used, combined with the morphological properties of the eye. The system showed an accuracy of 80.4% on 100 images. Li et al. (Li and Chutatape, 2004) presented a model based approach in which an snake was used to extract the vascular tree based on the location of the optic disk. Then, the information from the snake was used to find the macula center. The authors reported a 100% accuracy for optic disk localization and 100% for macula localization in 89 digital retinal images.

This paper presents an algorithm for the automatic localization and segmentation of the optic nerve head,

Mariño C., G. Penedo M., Pena S. and González F. (2008).
CREST LINES AND CORRELATION FILTER BASED LOCATION OF THE MACULA IN DIGITAL RETINAL IMAGES.
In *Proceedings of the First International Conference on Bio-inspired Systems and Signal Processing*, pages 521-527
DOI: 10.5220/0001066305210527

macula and fovea working on digital retinal fundus images. The optic nerve head is located and its shape is extracted without user intervention. Localization is achieved by means of a two stage process. In the first stage, creases are extracted and filtered, so that only the crest lines corresponding to the main vessel arc are not removed. Then a polynomial curve is fitted to the points in the crest lines, which will determine an area of interest where the optic disk will be located. In the second stage the shape of the optic disk is determined through the combination of two techniques: morphological operators and a deformable model. The final result is the optic disk shape and position. Once the optic disk position has been determined, macula and fovea are located using the morphological properties of the eye, which allow for the optimization of the search procedure, performed by means of a multi-scale correlation filter searching over a small area.

The setup of the paper is as follows. Section 2 provides details on the algorithm for the optic disk localization and segmentation. Section 3 describes the macula segmentation process. Experiments and results are given in section 4 for both the optic disk and macula localization and segmentation, and finally section 5 provides discussion and conclusions.

2 OPTIC DISK SEGMENTATION

The first stage of the process consists of locating the region where the optic disk is situated. This is performed by tracking the main crest lines, which converge in the optic disk. Then an accurate segmentation of the optic disk is obtained by means of a deformable model. This information, combined with the morphological properties of the eye, will be very useful in the process of locating and segmenting the macula.

2.1 Optic Disk Location

Analyzing the morphology of the retinal vessel tree (Figure 1), it is clear that the root of this tree is the optic disk, so by tracking the main vessels it is possible to arrive to the optic disk position. Following this approximation, an algorithm has been designed to obtain that position without the need of segmenting the whole retinal vessel tree.

Since the segmentation of the retinal vessel tree would be a costly process, only the crest lines of the main vessel arc are used in the detection of the optic disk position. To compute the crest lines, a geometric approach was used, the Multi-local Level Set

Figure 1: Digital retinal image acquisition. Note the convergence of the main vessels in the optic disk, fact which will be used in the detection of the optic disk position.

Extrinsic Curvature with the Structure Tensor filtering process (MLSEC-ST) (A. Lpez and Villanueva, 2000; Mariño et al., 2006). Using this method only the highest creases are preserved, and the main vessel arc creases are obtained, as shown in Figure 2.

However, in some of the images the crest lines obtained do not reach the optic disk due to the high filter levels applied, and it is necessary an interpolation method to compute the position of the optic disk (Figure 2, bottom). Analyzing the shape of the vessel arc, a parabolic fitting to the points in the creases seems to be the best approximation. But, from the results obtained, the two degree polynomial fitting showed to be inaccurate and a third level polynomial fitting was tried with satisfactory results. To obtain this curve, a least square fitting process was performed with the classic equation 1 and minimizing the expression in equation 2. In Figure 3 two examples of the result from the fitting process are depicted, with blue lines representing the curves interpolated from the crest lines.

$$y = ax^3 + bx^2 + cx + d \quad (1)$$

$$\sum_{i=1}^{n} [y_i - f(x_i)]^2 = \sum_{i=1}^{n} [y_i - (ax_i^3 + bx_i^2 + cx_i) + d]^2 \quad (2)$$

Once the optic disc is roughly located, an area of interest containing the optic disk is determined. This area will be centered in the coordinates where both branches of the main vessel arc crest lines converge, and its size will be two times the average optic disk size of all the images analyzed, so that every optic disk will be contained within this small area (the red rectangle in Figure 3). It is within this area where

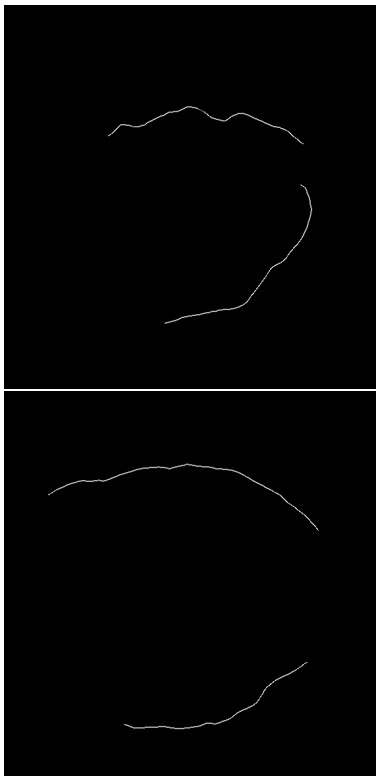

Figure 2: Crest lines obtained with the MLSEC-ST method. Top: crest lines reach the optic disk, so that its position is easily determined. Bottom: in some images, an interpolation method is necessary to reach the optic disc position.

the segmentation process will be performed, obtaining the shape and size of the optic disk.

2.2 Optic Disk Segmentation

Many works about the optic disk segmentation can be found in literature. Several methods were tried with the retinal images we are working with. The best results have been obtained with a deformable model-based segmentation process, based on the work by Hu et al. (Hu et al., 1998; Mariño et al., 2007). In this method, the deformable model is composed of a global model and a local model. The global model approximately fits the boundary of the optic disc. The local deformable model can get a more accurate fit to the characteristics of the boundary, keeping at the same time the shape of the model when the boundary does not exist or it is difficult to get. Optic disc segmentation is performed in three stages: in the first two stages the global model is fitted to the optic disc. In the third stage, starting from the result of the previous stages, the local model is accurately fitted to the particularities of the optic disk boundary. In Figure 4 two segmentation results are depicted, showing the accuracy of the method.

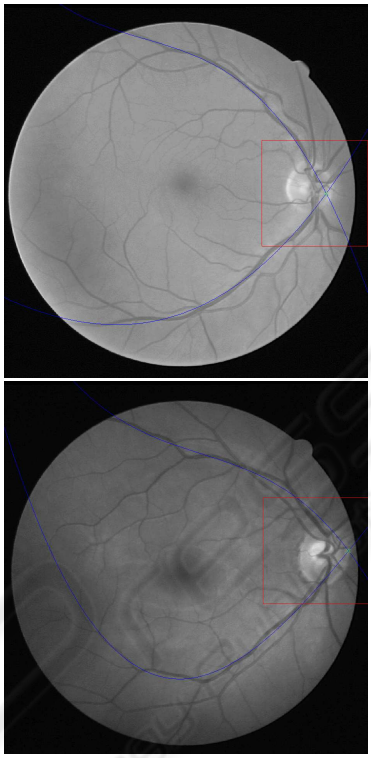

Figure 3: Results obtained from the third degree polynomial fitting applied to two different images. Blue lines represent the third degree polynomic curves fitted to the points of the creases.

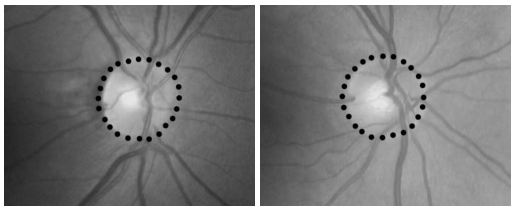

Figure 4: Results obtained from the segmentation process using the deformable model applied to two different retinal images.

Not that the optic disk has been located, the next step consists in licating the macula and fovea using the properties of the eye's morphology.

3 MACULA AND FOVEA DETECTION

The fovea is a small depression on the eye fundus. It is the darkest part in most of the retinal images, while

it is not obvious in some images due to high illumination or being covered by lesions. Its geometrical relation to other structures is employed to locate robustly the fovea. The method performs in two steps: first, a candidate area containing the macula is obtained, then, the macula size and position is located within this area through a matched filter.

3.1 Macula Candidate Region Selection

The candidate region for the fovea is defined as a circular area. Its center is located approximately at 2 disk diameters away from the optic disk center and its radius equals to the optic disk radius. Because the fovea is located about 2 times optic disk size temporal to the optic disk in the retinal images (Larsen, 1976), the candidate region is such defined in order to ensure that the fovea is within the region.

Since in section 2.2 we have computed the coordinates and diameter of the optic disk center, it is possible to obtain an accurate estimation of the fovea and macula position, by fitting a new parabolic curve to the main vessel arc, and taking the coordinates of the optic disk center as the parabola vertex. Following the work from Li et al. (Li and Chutatape, 2004), the parabolic shape is given by equation 3.

$$\begin{aligned}[(x-x_c)\sin\theta+(y-y_c)\cos\theta]^2 = \\ 2p[(x-x_c)\cos\theta-(y-y_c)\sin\theta]\end{aligned} \quad (3)$$

where x_c, y_c are the vertex coordinates, x and y are the searched points, $p/2$ represents the focal length, and θ is the rotation angle of the directrix. Then a search by mean square error is performed. In this work the shape of the curve has been represented by the general form given by equation 4, much simpler and computationally more efficient.

$$y = ax^2 + bx + c \quad (4)$$

Although in equation 4 the rotation and the parabolic vertex are not represented, the least square error fitting is a very simple process. Vertex coordinates can be computed using equation 5.

$$\begin{aligned}x_v &= -b/2a \\ y_v &= c - b^2/4a\end{aligned} \quad (5)$$

where x_v, y_v are the coordinates of the vertex. If we impose the restriction that the vertex will always be the center of the optic disk, combining equations 4 and 5 the parabola will be given by equation 6, defined by the parameter a and the optic disk center coordinate, already known from the previous segmentation stage.

$$\begin{aligned}b &= -2x_v a \\ c &= ax_v^2 + y_v\end{aligned} \quad (6)$$

Figure 5 represents the parabolic fitting process.

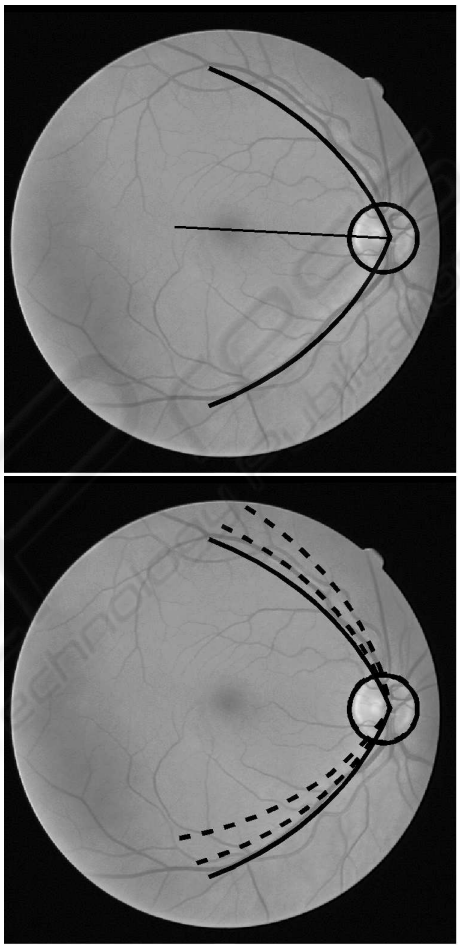

Figure 5: Representation of the parabolic model. Top: parabolic model with the directrix. Bottom: several iterations of the parabolic model searching for the best fit to the main arc vessels.

This way, following the parabola bisection two diameters away from the optic disk center, a search area can be defined, greatly reducing the search space where the macula is located. Figure 6 represents the process of determining this area of interest.

3.2 Fovea Location

Once the candidate area containing the macula has been located, a correlation filter is applied to the region in order to locate the macula and the fovea.

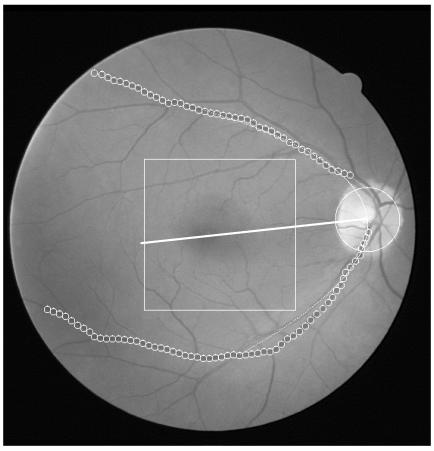

Figure 6: Computation of the candidate foveal region. Points from the creases (white circles) are fitted to the parabolic model and then, following the parabola directrix a fixed distance, the macula candidate search area is determined.

As previously stated, the fovea is a spot located in the center of the macula, and is responsible for the sharp central vision. The macula is commonly visible as a hazy dark area. To locate this dark area, a matched filter which consists of a Laplacian of Gaussian is used. The correlation filter is shown in Figure 7. The fovea will be located at the position where the response of the filter is maximum.

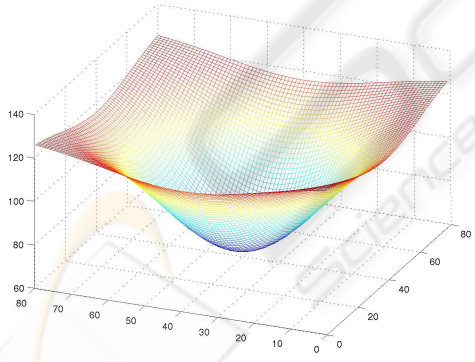

Figure 7: The correlation filter to locate the macula, where the template consists of a Laplacian of Gaussian.

The template is correlated with the intensity component of the retinal image. We use the full Pearson-R correlation to take variations in mean, intensity and contrast into account, as defined in Equation 7. The size of the filter is taken the same as the optic disk radius, since the diameter of the macula is about the same as the diameter of the optic disk (Larsen, 1976).

$$C_{i,j} = \frac{\sum_{x,y}(f(x,y) - \bar{f}(x,y))(w(x-i,y-j) - \bar{w})}{\sum_{x,y}(f(x,y) - f(x,y))^2 \sum_{x,y}(w(x-i,y-j) - \bar{w})^2} \quad (7)$$

The region of interest containing the macula is defined as an $n \times m$ rectangle whose center is the point with the higher response computed by means of the correlation filter. Figure 8 shows the result obtained by the macula segmentation process. The macula is marked as a white circle about the center of the image, while the fovea is marked with a cross in its center (optic disk segmentation result is also included, with its center marked as a red cross).

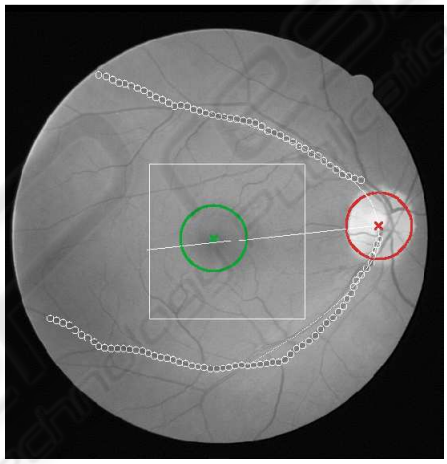

Figure 8: Result obtained by the macula segmentation process using the correlation matched filter in the image in Figure 6. Optic disk radius and center are marked in red, and fovea and macula contours are marked in green.

4 RESULTS

In order to test the accuracy of the method, several experiments have been designed, and the results have been validated by clinicians from the Complejo Hospitalario Universitario de Santiago (CHUS). The set of test images was composed of 135 retinal digital images with a resolution of 565×584 pixels. Table 1 contains the statistics for the test images, with average horizontal and vertical diameters of the optic disks (first and second column) and horizontal vs. vertical ratio (third column). This values will be used in the initialization stages of the deformable model, and will determine the size of the region of interest where the macula is located.

The main goal of this work is the macula location, and this task has been performed in two stages:

Table 1: Statistics (average, standard deviation, maximum and minimum) for the horizontal, vertical and ratio of the horizontal and vertical diameters (*horizontal/vertical*) for the images in the test set.

	Horizontal diameter	*Vertical diameter*	*Ratio Ratio*
Average	78,97	85,03	1,08
Standard deviation	7,34	8,36	0.09
Maximum	103	112	1,23
Minimum	65	70	0,77

the former determined an area of interest where the fovea will be searched, and in the latter the macula was segmented by means of a correlation filter. The results from the first stage are included in table 2. The location is considered *good* when the macula entirely contained within the area of interest. *Acceptable* results show the number of maculas from the set of test images partially contained in the area. A result is considered *bad* when the macula is mostly outside the area of interest. It is clear how the algorithm successfully detected the area of interest surrounding the macula in the 100% of the images in the test set.

Table 2: Results of the determination of the area of interest containing the macula.

Area of interest		
Good	*Acceptable*	*Bad*
100%	0%	0%
100%		0%

In the last stage of the process, the macula was segmented using a correlation filter. This process is very fast since the area where the search takes place is very small. Following the criteria of Goldbaum et al. (Goldbaum et al., 1996), there are three possible results in the segmentation:

1. *Good localization*: estimated center and real center (determined by an expert clinician) of the macula overlap.
2. *Acceptable localization*: estimated and real centers are not separated more than a mean radius (from table 1).
3. *Bad localization*: otherwise.

Following this categorization, the results obtained are depicted in table 3.

Figure 9 shows the results obtained in three different retinal images. The optic disk, the region containing the macula, the macula and the fovea have been marked in all of these images, showing the results commented in tables 2 and 3.

Table 3: Results for the macula location.

Macula location		
Good	*Acceptable*	*Bad*
97%	0%	3%
97%		3%

Table 4: Execution times for each one of the algorithm stages.

Stage	**Time (seconds)**
Creases extraction	0.537s
3rd. degree polynomic fit	0.020s
Optic disk segmentation	2.588s
Parabolic fit	0.033s
Macula location	0.324s
Total	3.502s

Finally, table 4 whows the execution times of each stage, from the creases computation to the macula location. These times were measured in a PIV 2.0GHz. From these times it is clear that a screening process involving thousands of people, which usually would take much time to the clinicians, could be greatly reduced with the help of a system like the one proposed in this paper.

5 CONCLUSIONS AND FURTHER WORK

In this work a methodology to locate and segment the optic disk and the macula has been presented. The algorithm performs in several stages, from the creases extraction, necessary for the optic disk location, to the macula location. Besides, high level domain knowledge is used to reduce the area where the macula is located once the optic disk has been detected. Still much work has to be done to improve the results of the process. A pyramidal search is being tried to obtain a better segmentation of the macula, and a higher number of images is necessary to validate the presented results. Moreover, tests with standard sets of images (like the DRIVE project (Staal et al., 2004)) need to be performed to obtain more reliable result statistics.

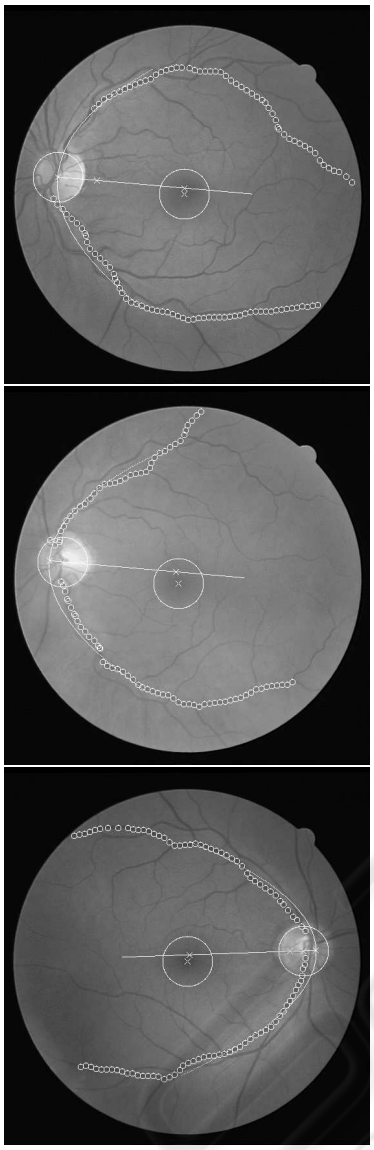

Figure 9: Results of the segmentation of the optic disk and the macula. These images show the results in three cases where the macula and optic disk were successfully located and segmented.

ACKNOWLEDGEMENTS

This paper has been partly funded by the Xunta de Galicia through the grant contract PGIDIT05SIN001E.

REFERENCES

A. Lpez, D. Lloret, J. S. and Villanueva, L. (2000). Multilocal creaseness based on the level set extrinsic curvature. *Computer Vision and Image Understanding*, 77:111–114.

Chanwimluang, T. and Fan, G. (2004). An efficient algorithm for extraction of anatomical structures in retinal images. *IEEE International Conference on Image Processing*, 23:1093–1096.

Goldbaum, M., Moezzi, S., Taylor, A., Chatterjee, S., Boyd, J., Hunter, E., and Jain, R. (1996). Automated diagnosis and image understanding with object extraction, object classification, and inferencing in retinal images. In *Proceedings of the International Conference on Image Processing*, volume 3, pages 695–698.

Hu, Y.-L., Rogers, W. L., Coast, D. A., Kramer, C. M., and Reicheck, N. (1998). Vessel boundary extraction based on a global and local deformable physical model with variable stiffness. *Magnetic Resonance Imaging*, 16:943–951.

Lalonde, M., Beaulieu, M., and Gagnon, L. (2001). Fast and robust optic disk detection using pyramidal decomposition and hausdorff–based template matching. *IEEE Transaction on Medical Imaging*, 20:1193–1200.

Larsen, H. W. (1976). *The Ocular Fundus: A Color Atlas*. Munksgaard.

Li, H. and Chutatape, O. (2004). Automated feature extraction in color retinal images by a model based approach. *IEEE Transactions on Medical Imaging*, 51(2):246–254.

Lowell, J., Hunter, A., Steel, D., Basu, A., Ryder, R., Fletcher, E., and Kennedy, L. (2004). Optic nerve head segmentation. *IEEE Transactions on medical Imaging*, 23:256–264.

Mariño, C., Barreira, N., Penedo, M. G., Ortas, M., Doncel, J. L., and Gómez-Ulla, F. (2007). Two stages optic disc segmentation in digital retinal images. *WSEAS Transactions on Information Science and Applications*, 4(4):771–778.

Mariño, C., Penedo, M. G., Penas, M., Carreora, M. J., and González, F. (2006). Personal authentication using digital retinal images. *Pattern Analysis and Applications*, (9):21–33.

Mendels, F., C., H., and J.P., T. (1999). Identification of the optic disk boundary in retinal images using active contours. *Proceedings of the Irish Machine Vision and Image Processing Conference*, pages 103–115.

Pinz, A., Bernögger, S., Datlinger, P., and Kruger, A. (1998). Mapping the human retina. *IEEE Transactions on Medical Imaging*, 17(4):606–619.

Sinthanayothin, C., Boyce, J., Cook, H., and Williamson, T. (1999). Automated localisation of the optic disc, fovea and retinal blood vessels from digital colour fundus images. *British Journal of Ophthalmology*, 83:902–910.

Staal, J., Abramoff, M., Niemeijer, M., Viergever, M., and van Ginneken, B. (2004). Ridge based vessel segmentation in color images of the retina. *IEEE Transactions on Medical Imaging*, 23:501–509. See also `http://www.isi.uu.nl/Research/Databases/DRIVE/`.